IEEE Access
Multidisciplinary : Rapid Review : Open Access Journal

Received June 21, 2019, accepted June 30, 2019, date of publication July 10, 2019, date of current version August 12, 2019.

Digital Object Identifier 10.1109/ACCESS.2019.2927810

Finite-Time Trajectory Tracking Control for Uncertain Underactuated Marine Surface Vessels

LEI ZHANG, BING HUANG, YULEI LIAO, AND BO WANG
Science and Technology on Underwater Vehicle Laboratory, Harbin Engineering University, Harbin 150001, China

Corresponding author: Bing Huang (binhuang@mail.nwpu.edu.cn)

This work was supported in part by the Fundamental Research Funds for the Central Universities under Grant GK2010260307, in part by the National Natural Science Foundation of China under Grant 51509054, Grant 51779052, and Grant 51709065, and in part by the Innovation Special Zone of National Defense Science and Technology.

ABSTRACT This paper concerns the finite-time trajectory tracking control problem for an underactuated marine surface vessel (MSV) suffering from the external disturbance and parameter uncertainties. First, the virtual velocity command is proposed based on a novel piecewise function. It will be illustrated that the position tracking error can be stabilized to small regions in finite time once the desired velocity commands are tracked. Then, an adaptive tracking controller is developed such that sway and yaw velocities can converge to the desired ones in finite time. Utilizing the proposed control strategy, global finite-time stability can be ensured for the position and velocity tracking errors even in the presence of external disturbances and parameter uncertainties. Finally, the effectiveness of the proposed controller is illustrated by numerical simulation.

INDEX TERMS Underactuated surface vessel, finite-time control, sliding mode control, trajectory tracking control.

I. INTRODUCTION

In recent years, trajectory tracking control for marine surface vessels (MSVs) has emerged as one of the most attractive fields due to its potential applications in various marine missions, involving environment monitoring, polar science research, rescue missions, etc. As one of the indispensable parts during these marine activities, trajectory tracking control always plays an important role to accomplish complicated tasks. However, designing controllers for MSVs still poses many challenges stemming from its highly nonlinear dynamics and underactuated characteristic. The underactuated characteristic means that the dimension of the control input of MSVs is always less than that of the configuration vector, leading to the non-integrable acceleration constraints on the sway dynamics. Furthermore, the complex ocean environment always produces unknown disturbance, such as wind and ocean current, making it a difficult task to track a desired trajectory. In spite of these difficulties, diverse advanced methods have been presented to design controllers for MSVs, such as adaptive control [1]–[3], backstepping control [4]–[6], sliding mode control [10], [11], fuzzy control [12], [13] and Neural Networks control [11]–[12].

The associate editor coordinating the review of this manuscript and approving it for publication was Liang Hu.

Considering the complex external disturbances and parameter uncertainties, adaptive control strategies have been widely adopted to developed controllers for MSVs by estimating unknown parameters online [1]–[3]. Compared with other nonlinear methods, sliding mode control strategy possesses better control performance in dealing with the external disturbances and system uncertainties [7]–[9], which leads to fruitful results for the trajectory tracking control of MSVs [10], [11]. Though, the external disturbance and uncertainties can be dealt with properly by the methods mentioned above, the unmodeled system dynamics should be taken into account. In view of this, Fuzzy control strategies [12] and Networks control approaches [13] have been exploited to approximate the uncertainties in system dynamics. A common problem in [1]–[13] is that the presented controllers can only be applied to fully actuated MSVs, leading to much limitation in practice.

To improve the applicability of the trajectory tracking controllers, ever-increasing focus is lying on the nonlinear control for underactuated MSVs. In [14], a liner sliding mode control scheme was constructed to deal with the lateral motion control of underactuated MSVs. In contrast to the proposed technology in [14], nonlinear sliding mode surfaces were designed to solve the tracking control problem for MSVs, which can effectively improve the convergence speed

[31]. However, the external disturbance has been ignored in [14] and [31], causing substantial performance degradation in practice. In order to reduce the adverse effect of the external disturbances and unmodeled system dynamics, a novel trajectory tracking control algorithm was proposed for underactuated autonomous underwater vehicles based on integral sliding mode control and neural network approach [16]. It must be noted that the transient and steady-state response of MSVs system cannot be prespecified in [14]-[16], though the external disturbance can be handled. Taking this fact into account, the prescribed performance control strategy and Barrier Lyapunov function have been investigated for tracking control of MSVs [17]–[20]. It is obvious that the proposed results can only be used to solve the tracking control problem of a single MSV. For the formation tracking control problem of multiple underactuated MSVs, researchers have acquired extremely abundant achievements [21]–[25].

Though effective for trajectory tracking control of underactuated MSVs, controllers proposed in [14]–[25] are asymptotically stable, meaning that the tracking error will be stabilized as time goes infinite. Compared with these asymptotically stable control schemes, finite-time control strategies for MSVs [26]–[29] possess faster convergence rate and better robustness to the external disturbance. By utilizing finite-time extended state observers, a distributed formation control strategy was established for multiple MSVs in [26]. In [27], a robust finite-time output feedback controller was proposed for MSVs based on a novel disturbance observer. For the purpose of improving the reliability of the MSVs system, a finite-time fault-tolerant control strategy was designed with LOS range and angle constraints considered [28]. A novel fixed-time output feedback trajectory tracking controller was proposed for MSVs subject to external disturbances and uncertainties [29]. It must be pointed out that these finite-time controllers proposed in [26]–[29] can only be applied to fully actuated MSVs. Therefore, it is highly desirable to design robust finite-time tracking controllers for underactuated MSV systems.

Motivated by the above observations, the finite-time trajectory tracking control problem for uncertain underactuated MSVs will be investigated by utilizing sliding mode technology and adaptive laws. The originality and novelty of the proposed control scheme are stated as follows:

i) Global finite-time stability can be ensured for the tracking errors of underactuated MSV systems even in the presence of external disturbances and parameter uncertainties. Different from the existing finite-time controllers presented in [26]–[29], the proposed controller in this paper can be used for underactuated MSVs, which is of great practical significance in engineering applications.

ii) Compared with the sliding mode methods given in [14] and [15], the external disturbance and system parameter uncertainties can be properly handled simultaneously, thus improving the practicality of the controller greatly.

iii) A novel finite-time sliding mode surface is established based on the hyperbolic tangent function. In contrast to the existing terminal sliding mode technology, the proposed method can avoid the singularity problem. Meanwhile, a novel adaptive law is constructed to ensure global finite-time stability for the sliding mode surface.

The remainder of this paper is given as follows. In section II, preliminaries and problem formulation are presented. Section III is devoted to controller design and stability analysis. In section IV, numerical simulations are conducted to show the effectiveness of the proposed controller. Finally, it comes to the conclusion of this paper in section V.

II. PRELIMINARIES AND PROBLEM FORMULATION

A. PRELIMINARIES

Notation. In this paper, the notation $|\sigma|$ represent the absolute value of a scalar σ, $\text{sig}^{\alpha}(\sigma)$ is defined as $\text{sig}^{\alpha}(\sigma) = |\sigma|^{\alpha}\,\text{sign}(\sigma)$.

Lemma 1 [30]: For the system $\dot{x} = f(x), f(0) = 0, x \in R^n$, $V(x)$ converges to the equilibrium point in finite time if there exists a continuous function $V(x) : U \to R$ satisfying Eq. (1), where $\gamma_1 > 0, \gamma_2 > 0, 0 < \gamma_3 < 1$.

$$\dot{V}(x) + \gamma_1 V(x) + \gamma_2 V^{\gamma_3}(x) \leq 0 \tag{1}$$

Lemma 2 [30]: For any scalar z_i, $i = 1, 2, \ldots, n$, equation (2) always holds when $0 < p < 1$ exists.

$$\sum_{i=1}^{n} |z_i|^{1+p} \geq \left(\sum_{i=1}^{n} |z_i|^2\right)^{\frac{1+p}{2}} \tag{2}$$

Lemma 3 [5]: For any $z \in R$, $\mu > 0$ and $\kappa = 0.2785$, the relation Eq. (2) exists.

$$0 < |z| - z\tanh(\mu z) \leq \frac{\kappa}{\mu} \tag{3}$$

B. DYNAMIC MODEL OF AN UNDERACTUATED SURFACE VESSEL

The kinematic and dynamic model of an uncertain underactuated MSV with three degree of freedom is established in this section. Assuming that the MSV moves in the horizontal plane, its kinematic mathematical model can be written as [15]:

$$\begin{cases} \dot{x} = u\cos(\psi) - v\sin(\psi) \\ \dot{y} = u\sin(\psi) + v\cos(\psi) \\ \dot{\psi} = r \end{cases} \tag{4}$$

where x and y denote the surge and sway displacement of the center of mass, respectively, ψ denote the yaw angle of the MSV defined in the earth-fixed frame, u, v and r stand for the surge, sway and yaw angular velocity with respect to the body-fixed frame, respectively.

The dynamic model of the MSV with external disturbances can be given as [15]:

$$\begin{cases} m_{11}\dot{u} - m_{22}vr + d_{11}u = \tau_u + \tau_{ud} \\ m_{22}\dot{v} + m_{11}ur + d_{22}v = \tau_{vd} \\ m_{33}\dot{r} + (m_{22} - m_{11})\,uv + d_{33}r = \tau_r + \tau_{rd} \end{cases} \tag{5}$$

with $d_{11}, d_{22}, d_{33}, m_{11}, m_{22}, m_{33}$ being the hydrodynamic damping and ship inertia including added mass in surge, sway and yaw, τ_u and τ_r being the surge force and the yaw moment, τ_{ud}, τ_{vd} and τ_{rd} being the unknown external disturbances.

To derive the finite-time trajectory tracking controller for the MSV, the following assumptions are introduced.

Assumption 1: The external disturbance always satisfies $|\tau_{ud}| \leq D_1, |\tau_{vd}| + |\dot{\tau}_{vd}| \leq D_2, |\tau_{rd}| \leq D_3$ with D_1, D_2 and D_3 being positive constants.

Assumption 2: The reference trajectories x_d, y_d and their derivatives are always bounded.

C. TRACKING ERROR DYNAMICS

Defining the tracking errors x_e, y_e, e_u and e_v as $x_e = x - x_d$,$y_e = y - y_d$, $e_u = u - u_d$ and $e_v = v - v_d$, respectively, where u_d and v_d are desired surge and sway velocity, respectively, the error dynamics can be established as Eqs. (6)-(7) by combining the kinematic model Eq. (4) and the dynamic model Eq. (5).

$$\begin{bmatrix} \dot{x}_e \\ \dot{y}_e \end{bmatrix} = \begin{bmatrix} \cos\psi & -\sin\psi \\ \sin\psi & \cos\psi \end{bmatrix} \begin{bmatrix} u \\ v \end{bmatrix} - \begin{bmatrix} \dot{x}_d \\ \dot{y}_d \end{bmatrix} \tag{6}$$

$$\begin{cases} \dot{e}_u = \dfrac{1}{m_{11}} (\delta_u \tau_u + \tau_{ud} + m_{22} v r - d_{11} u) - \dot{u}_d \\ \dot{e}_v = -\dfrac{1}{m_{22}} (m_{11} u r + d_{22} v - \tau_{vd}) - \dot{v}_d \end{cases} \tag{7}$$

D. PROBLEM FORMULATION

Finite-time trajectory tracking control problem for USVs refers to design controllers such that the vehicle's position can converge to the desired ones in the presence of external disturbance and parameter uncertainties, that is, $\lim_{t \to T} |x_e| \leq \Delta_x$, $\lim_{t \to T} |y_e| \leq \Delta_y$, where Δ_x and Δ_y are small positive constants, $x_e = x - x_d$,$y_e = y - y_d$.

III. CONTROLLER DESIGN

In this section, a finite-time controller is developed to realize the control objective. Initially, novel desired velocity commands u_d and v_d will be proposed to ensure finite-time stability for the tracking errors x_e and y_e. In the further design, x_e and y_e will be stabilized to small regions Δ_x and Δ_y only if the sway and yaw velocity can converge to the desired trajectory. To this end, an adaptive finite-time controller is proposed such that the sway and yaw velocity can converge to the desired velocity commands. Thus, the controller design procedure is twofold. In the first step, the desired velocity is proposed by utilizing a novel piecewise function. In the second step, a finite-time controller is developed based on the sliding mode control method.

A. DESIRED VELOCITY DESIGN

Theorem 1. Considering the position tracking error dynamic Eq. (6), if the velocity tracking errors e_u and e_v converge to two small residual sets Δ_u and Δ_v in finite time, respectively, the position tracking errors x_e and y_e will converge to small regions Δ_x and Δ_y in finite time when the desired surge and sway velocity are proposed as Eqs. (8)-(10).

$$\begin{bmatrix} u_d \\ v_d \end{bmatrix} = \begin{bmatrix} \cos\psi & \sin\psi \\ -\sin\psi & \cos\psi \end{bmatrix} \begin{bmatrix} \dot{x}_d - k_1 H(x_e) \\ \dot{y}_d - k_2 H(y_e) \end{bmatrix} \tag{8}$$

$$H(z) = \begin{cases} z + |z|^\alpha \operatorname{sign}(z), |z| > \Delta, & z = x_e, y_e \\ z + \dfrac{2\Delta}{\pi} \sin\left(\dfrac{\pi}{2\Delta} z\right) + \alpha \Delta^{\alpha - 1} z, & |z| \leq \Delta \end{cases} \tag{9}$$

$$\Delta = (\frac{\pi}{2}(1-\alpha))^{\frac{1}{1-\alpha}} \tag{10}$$

$$\Delta_x = \min\left(\Delta, \frac{o}{\sqrt{k_1 - \frac{1}{4}}}, \sqrt[\alpha+1]{\frac{o^2}{k_1}}\right)$$

$$\Delta_y = \min\left(\Delta, \frac{o}{\sqrt{k_2 - \frac{1}{4}}}, \sqrt[\alpha+1]{\frac{o^2}{k_2}}\right) \tag{11}$$

Here, α, k_1, k_2 and o are positive constants satisfying $0 < \alpha < 1$, $k_1 > \frac{1}{4}$, $k_2 - \frac{1}{4}$, $o = \sqrt{\Delta_u^2 + \Delta_v^2}$.

Proof: The Lyapunov function is selected as:

$$V_1 = \frac{1}{2} x_e^2 \tag{12}$$

According to Eq. (6), the following equation can be obtained:

$$\begin{bmatrix} u \\ v \end{bmatrix} = \begin{bmatrix} \cos\psi & \sin\psi \\ -\sin\psi & \cos\psi \end{bmatrix} \begin{bmatrix} \dot{x} \\ \dot{y} \end{bmatrix} \tag{13}$$

According to the definition of the velocity tracking error e_u and e_v, the following equation can be derived by combing Eq. (8) and Eq. (13).

$$\begin{bmatrix} e_u \\ e_v \end{bmatrix} = \begin{bmatrix} \cos\psi & \sin\psi \\ -\sin\psi & \cos\psi \end{bmatrix} \begin{bmatrix} \dot{x}_e + k_1 H(x_e) \\ \dot{y}_e + k_2 H(y_e) \end{bmatrix} \tag{14}$$

For clarity, we define $\boldsymbol{A} = [e_u; e_v]$, $\boldsymbol{B} = \begin{bmatrix} \cos\psi & \sin\psi \\ -\sin\psi & \cos\psi \end{bmatrix}$, $\boldsymbol{C} = [\dot{x}_e + k_1 H(x_e); \dot{y}_e + k_2 H(y_e)]$, Due to the fact that $\|\boldsymbol{A}\| \leq o$, $\|\boldsymbol{B}\| = 1$, it can be concluded from Eq. (14) that $\|\boldsymbol{C}\| \leq o$. Thus, the following relation can be deduced:

$$\begin{cases} \dot{x}_e + k_1 H(x_e) \leq o \\ \dot{y}_e + k_2 H(y_e) \leq o \end{cases} \tag{15}$$

Differentiating V_1 with respect to time and substituting Eq. (15) yield

$$\begin{aligned} \dot{V}_1 &= x_e \dot{x}_e \\ &\leq -x_e (k_1 H(x_e) - o) \end{aligned} \tag{16}$$

Recalling the definition of $H(x_e)$ by Eq. (9), it leads to the following result if $|x_e| > \Delta$ exists.

$$\begin{aligned} \dot{V}_1 &\leq -x_e \left(k_1 |x_e|^\alpha \operatorname{sign}(x_e) + k_1 x_e - o\right) \\ &= -k_1 |x_e|^{\alpha+1} - k_1 x_e^2 + x_e o \\ &\leq -k_1 \left(x_e^2\right)^{\frac{\alpha+1}{2}} - k_1 x_e^2 + \frac{1}{4} x_e^2 + o^2 \\ &= -k_1 \left(x_e^2\right)^{\frac{\alpha+1}{2}} - \left(k_1 - \frac{1}{4}\right) x_e^2 + o^2 \end{aligned} \tag{17}$$

To deal with the term o^2, Eq. (17) can be further written as Eqs. (18)-(19).

$$\begin{aligned}\dot{V}_1 &\leq -\left(k_1 - \frac{1}{4} - \frac{o^2}{x_e^2}\right) x_e^2 - k_1 \left(x_e^2\right)^{\frac{\alpha+1}{2}} \\ &= -2\left(k_1 - \frac{1}{4} - \frac{o^2}{x_e^2}\right) V_1 - 2^{\frac{\alpha+1}{2}} k_1 V_1^{\frac{\alpha+1}{2}} \\ &= -\rho_1 V_1 - \rho_2 V_1^{\frac{\alpha+1}{2}} \qquad (18) \\ \dot{V}_1 &\leq -\left(k_1 - \frac{1}{4}\right) x_e^2 - \left(k_1 - \frac{o^2}{|x_e|^{\alpha+1}}\right) \left(x_e^2\right)^{\frac{\alpha+1}{2}} \\ &= -2\left(k_1 - \frac{1}{4} - \frac{o^2}{x_e^2}\right) V_1 - 2^{\frac{\alpha+1}{2}} k_1 V_1^{\frac{\alpha+1}{2}} \\ &= -\rho_1 V_1 - \rho_2 V_1^{\frac{\alpha+1}{2}} \qquad (19)\end{aligned}$$

where $\rho_1 = 2\left(k_1 - \frac{1}{4} - \frac{o^2}{x_e^2}\right)$, $\rho_2 = 2^{\frac{\alpha+1}{2}} k_1$, $\rho_3 = 2\left(k_1 - \frac{1}{4}\right)$,$\rho_4 = 2^{\frac{\alpha+1}{2}}\left(k_1 - \frac{o^2}{|x_e|^{\alpha+1}}\right)$. Then, in view of Lemma 1, it can come to the conclusion that x_e will converge to the region $|x_e| \leq \min\left(\Delta, \frac{o}{\sqrt{k_1 - \frac{1}{4}}}, \sqrt[\alpha+1]{\frac{o^2}{k_1}}\right)$ in finite time if $\rho_1 > 0$, $\rho_2 > 0$, $\rho_3 > 0$, $\rho_4 > 0$.

Through a similar analysis, one can deduce that y_e will converge to the region $|y_e| \leq \min\left(\Delta, \frac{o}{\sqrt{k_2 - \frac{1}{4}}}, \sqrt[\alpha+1]{\frac{o^2}{k_2}}\right)$ in finite time.

Thus, Theorem 1 has been proven.

Remark 1: Compared with the existing works [14] and [15], where the desired velocities u_d and v_d can only guarantee asymptotic convergence for the position tracking error x_e and y_e, finite-time stability can be obtained for x_e and y_e if the desired velocities are designed as Eqs (8)-(10). Consequently, the proposed algorithm possesses faster convergence ability than that in [14] and [15].

Remark 2: The nonlinear function $H(z)$ defined in Eq. (9) is applied to ensure finite-time stability for the position tracking errors. Though the singularity problem can be avoided, x_e and y_e can only converge into two small regions rather than the origin. The parameter Δ must be selected such that $H(z)$ be continuous and differentiable at the point $z = \Delta$. Thus, by assuming $H\left(\Delta^+\right) = H\left(\Delta^-\right)$ and $\dot{H}\left(\Delta^+\right) = \dot{H}\left(\Delta^-\right)$, Δ can be calculated as $\Delta = (\frac{\pi}{2}(1-\alpha))^{\frac{1}{1-\alpha}}$.

Remark 3. In order to facilitate the controllers design, the derivative of $H(z)$ is given as follows:

$$\dot{H}(z) = \begin{cases} \dot{z} + \alpha |z|^{\alpha-1} \dot{z}, |z| > \Delta, z = x_e, y_e \\ \dot{z} + \frac{2\Delta}{\pi} \cos\left(\frac{\pi}{2\Delta} z\right) \dot{z} + \alpha \Delta^{\alpha-1} \dot{z}, |z| \leq \Delta \end{cases} \qquad (20)$$

B. FINITE-TIME CONTROLLER DESIGN

In this subsection, an adaptive tracking controller will be developed to ensure finite-time stability for the velocity tracking errors. From theorem 1, it is concluded that x_e and y_e are finite-time stable only if e_u and e_v converge to two small regions under the desired velocity Eq. (8). Therefore, global finite-time stability will be derived for the position and velocity tracking errors under the proposed control scheme.

To pursue the control problem, two novel sliding mode surfaces are proposed as:

$$S_1 = e_u + k_3 \int_0^t \tanh(\kappa e_u)\, dt \qquad (21)$$

$$S_2 = \dot{e}_v + k_4 \tanh(\kappa e_v) \qquad (22)$$

where $k_3 > \frac{1}{4}, k_4 > \frac{1}{4}$. Recalling the definition of u_d and v_d in Eq. (8), $\dot{u}_d$, $\dot{v}_d$ and $\ddot{v}_d$ can be calculated as:

$$\begin{aligned}\begin{bmatrix}\dot{u}_d \\ \dot{v}_d\end{bmatrix} &= r \begin{bmatrix} -\sin\psi & \cos\psi \\ -\cos\psi & -\sin\psi \end{bmatrix} \begin{bmatrix} \dot{x}_d - k_1 H(x_e) \\ \dot{y}_d - k_2 H(y_e) \end{bmatrix} \\ &\quad + \begin{bmatrix} \cos\psi & \sin\psi \\ -\sin\psi & \cos\psi \end{bmatrix} \begin{bmatrix} \ddot{x}_d - k_1 \dot{H}(x_e) \\ \ddot{y}_d - k_2 \dot{H}(y_e) \end{bmatrix} \qquad (23) \\ &= r \begin{bmatrix} v_d \\ -u_d \end{bmatrix} + \begin{bmatrix} \cos\psi \sin\psi \\ -\sin\psi \cos\psi \end{bmatrix} \begin{bmatrix} \ddot{x}_d - k_1 \dot{H}(x_e) \\ \ddot{y}_d - k_2 \dot{H}(y_e) \end{bmatrix} \\ \ddot{v}_d &= -\dot{r} u_d + \Lambda \qquad (24)\end{aligned}$$

where

$$\begin{aligned}\Lambda &= -r\dot{u}_d - \left(\ddot{x}_d - k_1 \dot{H}(x_e)\right) r\cos\psi \\ &\quad - \left(\ddot{y}_d - k_2 \dot{H}(y_e)\right) r\sin\psi - \left(x_d - k_1 \ddot{H}(x_e)\right) \sin\psi \\ &\quad + \left(y_d - k_2 \ddot{H}(y_e)\right) \cos\psi \qquad (25)\end{aligned}$$

Thus, the derivative of S_1 and S_2 can be calculated as:

$$\begin{aligned}\dot{S}_1 &= \dot{e}_u + k_3 \tanh(\kappa e_u) \\ &= \frac{1}{m_{11}} \left(\delta_u \tau_u + \tau_{ud} + m_{22} v r - d_{11} u\right) - \dot{u}_d \\ &\quad + k_3 \tanh(\kappa e_u) \qquad (26) \\ \dot{S}_2 &= \ddot{e}_v + k_4 \left(1 - (\tanh(\kappa e_v))^2\right) \dot{e}_v \\ &= -\frac{1}{m_{22}} \left(m_{11} \dot{u} r + m_{11} u \dot{r} + d_{22} \dot{v} - \dot{\tau}_{vd}\right) \\ &\quad - \ddot{v}_d + k_4 \left(1 - (\tanh(\kappa e_v))^2\right) \dot{e}_v \\ &= -\frac{1}{m_{22}} \left(m_{11} \dot{u} r + d_{22} \dot{v} - \dot{\tau}_{vd}\right) - \left(\frac{m_{11}}{m_{22}} u - u_d\right) \dot{r} \\ &\quad - \Lambda + k_4 \kappa \left(1 - \tanh^2(\kappa e_v)\right) \dot{e}_v \qquad (27)\end{aligned}$$

It is worth pointing out that the sliding mode surface Eqs. (21) and (22) can ensure finite-time stability for tracking errors e_u and e_v. Specifically, these two tracking errors will converge to two small regions around the origin only if the sliding mode manifolds Eqs. (21) and (22) can be reached within finite time. Upon utilizing the proposed sliding mode surfaces, the following adaptive controllers can be designed:

$$\begin{aligned}\tau_u &= -m_{22} v r + d_{11} u + m_{11} \dot{u}_d - k_5 \mathrm{sign}(S_1) \\ &\quad - k_3 m_{11} \tanh(\kappa e_u) - \lambda_1 \tanh\left(\hat{D}_1\right) \mathrm{sign}(S_1) - k_7 S_1 \qquad (28) \\ \tau_r &= (m_{22} - m_{11})\, u v - \lambda_2 \tanh\left(\hat{D}_2\right) \mathrm{sign}(S_2) \\ &\quad - \lambda_3 \tanh\left(\hat{D}_3\right) \mathrm{sign}\left(\frac{(m_{22} u_d - m_{11} u)\, S_2}{m_{33}}\right)\end{aligned}$$

$$- \frac{m_{33}}{(m_{22}u_d - m_{11}u)} (m_{11}\dot{u}r + d_{22}\dot{v} + m_{22} (\Lambda - k_4\kappa \left(1 - \tanh^2 (\kappa e_v)\right) \dot{e}_v)) + d_{33}r - k_6 \text{sign} \left(\frac{(m_{22}u_d - m_{11}u) S_2}{m_{33}}\right) - k_8 S_2 \tag{29}$$

$$\dot{\hat{D}}_1 = \frac{\lambda_4}{\lambda_1} \cosh^2 \left(\hat{D}_1\right) |S_1| \tag{30}$$

$$\dot{\hat{D}}_2 = \frac{\lambda_5}{\lambda_2} \cosh^2 \left(\hat{D}_2\right) |S_2| \tag{31}$$

$$\dot{\hat{D}}_3 = \frac{\lambda_6}{\lambda_3} \cosh^2 \left(\hat{D}_3\right) \left|\frac{(m_{22}u_d - m_{11}u) S_2}{m_{33}}\right| \tag{32}$$

where k_5,k_6,λ_i, $i = 1, 2, \ldots, 6$ are positive constants, $\hat{D}_i$, $i = 1, 2, 3$ is the estimation of D_i, $i = 1, 2, 3$.

Remark 4: In control laws Eqs. (28) and (29), the hyperbolic tangent function is used to develop finite-time control laws. In this way, terms $\lambda_1 \tanh\left(\hat{D}_1\right) \text{sign}(S_1)$ and $\lambda_3 \tanh\left(\hat{D}_3\right)$ possess upper bounds, which depend on the design parameters λ_1 and λ_2. As a result, the output of the control laws will not approach to infinity despite the use of adaptive laws.

Theorem 2: Considering the MSV tracking error dynamic system represented by Eq. (7) satisfying Assumption 1 and Assumption 2, the following conclusions can be derived under the proposed control laws Eqs. (28)-(31).

i) The sliding mode surface $S_i, i = 1, 2$ will converge to the origin within finite time. Furthermore, the estimation errors $\tilde{D}_i = D_i - \lambda_i \tanh\left(\hat{D}_i\right), i = 1, 2, 3$ will be uniformly ultimately bounded.

ii) Tracking errors e_u and e_v will converge to regions Δ_u and Δ_v in finite time.

$$\Delta_u \leq \sqrt{2} (k_3 + k_4) \tag{33}$$

$$\Delta_v \leq \sqrt{2} (k_3 + k_4) \tag{34}$$

Proof: The overall Lyapunov function can be selected as

$$V_2 = \frac{1}{2}S_1^2 + \frac{1}{2}S_2^2 + \frac{1}{2\lambda_4}\tilde{D}_1^2 + \frac{1}{2\lambda_5}\tilde{D}_2^2 + \frac{1}{2\lambda_6}\tilde{D}_3^2 \tag{35}$$

Differentiating V_2 with respect to time and substituting Eqs. (7), (21), (22) and (27) yield

$$\begin{aligned}
\dot{V}_2 &= m_{11}S_1\dot{S}_1 + m_{22}S_2\dot{S}_2 - \frac{\lambda_1}{\lambda_4}\tilde{D}_1\frac{1}{\cosh^2\left(\hat{D}_1\right)}\dot{\hat{D}}_1 \\
&\quad -\frac{\lambda_2}{\lambda_5}\tilde{D}_2\frac{1}{\cosh^2\left(\hat{D}_2\right)}\dot{\hat{D}}_2 - \frac{\lambda_3}{\lambda_6}\tilde{D}_3\frac{1}{\cosh^2\left(\hat{D}_3\right)}\dot{\hat{D}}_3 \\
&= S_1 (\tau_u + \tau_{ud} + m_{22}vr - d_{11}u - m_{11}\dot{u}_d \\
&\quad + k_3m_{11} \tanh(\kappa e_u)) - S_2 (m_{11}\dot{u}r + d_{22}\dot{v} - \dot{\tau}_{vd} \\
&\quad - (m_{22}u_d - m_{11}u)\dot{r} + m_{22} (\Lambda - k_4\kappa (1- \\
&\quad \tanh^2(\kappa e_v)) \dot{e}_v)) - \frac{\lambda_1}{\lambda_4}\tilde{D}_1\frac{1}{\cosh^2\left(\hat{D}_1\right)}\dot{\hat{D}}_1 \\
&\quad - \frac{\lambda_2}{\lambda_5}\tilde{D}_2\frac{1}{\cosh^2\left(\hat{D}_2\right)}\dot{\hat{D}}_2 - \frac{\lambda_3}{\lambda_6}\tilde{D}_3\frac{1}{\cosh^2\left(\hat{D}_3\right)}\dot{\hat{D}}_3
\end{aligned}$$

$$\begin{aligned}
&\leq S_1 (\tau_u + m_{22}vr - d_{11}u - m_{11}\dot{u}_d \\
&\quad + k_3m_{11} \tanh(\kappa e_u)) - S_2 (m_{11}\dot{u}r + d_{22}\dot{v} \\
&\quad + m_{22}\left(\Lambda - k_4\kappa\left(1 - \tanh^2(\kappa e_v)\right)\dot{e}_v\right) \\
&\quad - \frac{(m_{22}u_d - m_{11}u)}{m_{33}}(\tau_r - (m_{22} - m_{11})uv - d_{33}r)\Big) \\
&\quad + |S_1| D_1 + |S_2| D_2 + \frac{|(m_{22}u_d - m_{11}u) S_2|}{m_{33}}D_3 \\
&\quad - \frac{\lambda_1}{\lambda_4}\tilde{D}_1\frac{1}{\cosh^2\left(\hat{D}_1\right)}\dot{\hat{D}}_1 - \frac{\lambda_2}{\lambda_5}\tilde{D}_2\frac{1}{\cosh^2\left(\hat{D}_2\right)}\dot{\hat{D}}_2 \\
&\quad - \frac{\lambda_3}{\lambda_6}\tilde{D}_3\frac{1}{\cosh^2\left(\hat{D}_3\right)}\dot{\hat{D}}_3
\end{aligned} \tag{36}$$

Based on the proposed control law Eqs. (28) and (29), Eq. (36) is further rearranged as

$$\begin{aligned}
\dot{V}_2 &\leq -k_5S_1\text{sign}(S_1) + |S_1| D_1 - \frac{\lambda_1}{\lambda_4}\tilde{D}_1\frac{1}{\cosh^2\left(\hat{D}_1\right)}\dot{\hat{D}}_1 \\
&\quad -\frac{k_6 (m_{22}u_d - m_{11}u) S_2}{m_{33}}\text{sign}\left(\frac{(m_{22}u_d - m_{11}u) S_2}{m_{33}}\right) \\
&\quad -\frac{\lambda_2}{\lambda_5}\tilde{D}_2\frac{1}{\cosh^2\left(\hat{D}_2\right)}\dot{\hat{D}}_2 - \frac{\lambda_3}{\lambda_6}\tilde{D}_3\frac{1}{\cosh^2\left(\hat{D}_3\right)}\dot{\hat{D}}_3 \\
&\quad -\lambda_1 \tanh\left(\hat{D}_1\right)|S_1| - \lambda_2 \tanh\left(\hat{D}_2\right)|S_2| \\
&\quad -\lambda_3 \tanh\left(\hat{D}_3\right)\left|\frac{(m_{22}u_d - m_{11}u) S_2}{m_{33}}\right| + |S_2| D_2 \\
&\quad +\frac{|(m_{22}u_d - m_{11}u) S_2|}{m_{33}}D_3 \\
&= -k_5 |S_1| - k_6\left|\frac{(m_{22}u_d - m_{11}u) S_2}{m_{33}}\right| \\
&\quad -\frac{\lambda_1}{\lambda_4}\tilde{D}_1\frac{1}{\cosh^2\left(\hat{D}_1\right)}\dot{\hat{D}}_1 - \frac{\lambda_2}{\lambda_5}\tilde{D}_2\frac{1}{\cosh^2\left(\hat{D}_2\right)}\dot{\hat{D}}_2 \\
&\quad -\frac{\lambda_3}{\lambda_6}\tilde{D}_3\frac{1}{\cosh^2\left(\hat{D}_3\right)}\dot{\hat{D}}_3 + |S_1|\tilde{D}_1 + |S_2|\tilde{D}_2 \\
&\quad + \left|\frac{(m_{22}u_d - m_{11}u) S_2}{m_{33}}\right|\tilde{D}_3
\end{aligned} \tag{37}$$

Upon applying Eqs. (30)-(32), Eq. (37) is rewritten as

$$\begin{aligned}
\dot{V}_2 &\leq -k_5 |S_1| - k_6\left|\frac{(m_{22}u_d - m_{11}u) S_2}{m_{33}}\right| \\
&\quad -\tilde{D}_1 |S_1| - \tilde{D}_2 |S_2| - \tilde{D}_3\left|\frac{(m_{22}u_d - m_{11}u) S_2}{m_{33}}\right| \\
&\quad + |S_1|\tilde{D}_1 + |S_2|\tilde{D}_2 + \left|\frac{(m_{22}u_d - m_{11}u) S_2}{m_{33}}\right|\tilde{D}_3 \\
&= -k_5 |S_1| - k_6\left|\frac{(m_{22}u_d - m_{11}u) S_2}{m_{33}}\right| \\
&\leq 0
\end{aligned} \tag{38}$$

Thus, the sliding mode surface S_i, $i = 1, 2$ and the estimation error $\tilde{D}_i$ are uniformly ultimately bounded.

In what follows, the finite time convergence of the tracking error and the sliding mode surface will be illustrated. By selecting positive constants $\bar{D}_i, i = 1, 2, 3$ satisfying $\bar{D}_i > D_i$ and $\bar{D}_i > \lambda_i \tanh\left(\hat{D}_i\right)$, the Lyapunov function is chosen as:

$$\begin{aligned} V_3 =& \frac{1}{2}S_1^2 + \frac{1}{\lambda_4}\left(\bar{D}_1 - \lambda_1 \tanh\left(\hat{D}_1\right)\right)^2 \\ &+ \frac{1}{2}S_2^2 + \frac{1}{\lambda_5}\left(\bar{D}_2 - \lambda_2 \tanh\left(\hat{D}_2\right)\right)^2 \\ &+ \frac{1}{\lambda_6}\left(\bar{D}_3 - \lambda_3 \tanh\left(\hat{D}_3\right)\right)^2 \end{aligned} \tag{39}$$

Differentiating V_3 by using Eqs. (7), (21), (22) and (27) yields

$$\begin{aligned} \dot{V}_3 =& m_{11}S_1\dot{S}_1 + m_{22}S_2\dot{S}_2 \\ &- \frac{2\lambda_1}{\lambda_4}\left(\bar{D}_1 - \lambda_1 \tanh\left(\hat{D}_1\right)\right)\frac{1}{\cosh^2\left(\hat{D}_1\right)}\dot{\hat{D}}_1 \\ &- \frac{2\lambda_2}{\lambda_5}\left(\bar{D}_2 - \lambda_2 \tanh\left(\hat{D}_2\right)\right)\frac{1}{\cosh^2\left(\hat{D}_2\right)}\dot{\hat{D}}_2 \\ &- \frac{2\lambda_3}{\lambda_6}\left(\bar{D}_3 - \lambda_3 \tanh\left(\hat{D}_3\right)\right)\frac{1}{\cosh^2\left(\hat{D}_3\right)}\dot{\hat{D}}_3 \\ =& S_1\left(\tau_u + \tau_{ud} + m_{22}vr - d_{11}u - m_{11}\dot{u}_d\right. \\ &\left.+ k_3 m_{11}\tanh\left(\kappa e_u\right)\right) - S_2\left(m_{11}\dot{u}r + d_{22}\dot{v} - \dot{\tau}_{vd}\right. \\ &- \left(m_{22}u_d - m_{11}u\right)\dot{r} + m_{22}\left(\Lambda - k_4\kappa\left(1 -\right.\right. \\ &\left.\left.\left.\tanh^2\left(\kappa e_v\right)\right)\dot{e}_v\right)\right) \\ &- \frac{2\lambda_1}{\lambda_4}\left(\bar{D}_1 - \lambda_1 \tanh\left(\hat{D}_1\right)\right)\frac{1}{\cosh^2\left(\hat{D}_1\right)}\dot{\hat{D}}_1 \\ &- \frac{2\lambda_2}{\lambda_5}\left(\bar{D}_2 - \lambda_2 \tanh\left(\hat{D}_2\right)\right)\frac{1}{\cosh^2\left(\hat{D}_2\right)}\dot{\hat{D}}_2 \\ &- \frac{2\lambda_3}{\lambda_6}\left(\bar{D}_3 - \lambda_3 \tanh\left(\hat{D}_3\right)\right)\frac{1}{\cosh^2\left(\hat{D}_3\right)}\dot{\hat{D}}_3 \\ \leq& S_1\left(\tau_u + m_{22}vr - d_{11}u - m_{11}\dot{u}_d\right. \\ &\left.+ k_3 m_{11}\tanh\left(\kappa e_u\right)\right) - S_2\left(m_{11}\dot{u}r + d_{22}\dot{v}\right. \\ &+ m_{22}\left(\Lambda - k_4\kappa\left(1 - \tanh^2\left(\kappa e_v\right)\right)\dot{e}_v\right) \\ &\left.- \frac{\left(m_{22}u_d - m_{11}u\right)}{m_{33}}\left(\tau_r - \left(m_{22} - m_{11}\right)uv - d_{33}r\right)\right) \\ &+ \left|S_1\right| D_1 + \left|S_2\right| D_2 + \frac{\left|\left(m_{22}u_d - m_{11}u\right)S_2\right|}{m_{33}}D_3 \\ &- \frac{2\lambda_1}{\lambda_4}\left(\bar{D}_1 - \lambda_1 \tanh\left(\hat{D}_1\right)\right)\frac{1}{\cosh^2\left(\hat{D}_1\right)}\dot{\hat{D}}_1 \\ &- \frac{2\lambda_2}{\lambda_5}\left(\bar{D}_2 - \lambda_2 \tanh\left(\hat{D}_2\right)\right)\frac{1}{\cosh^2\left(\hat{D}_2\right)}\dot{\hat{D}}_2 \\ &- \frac{2\lambda_3}{\lambda_6}\left(\bar{D}_3 - \lambda_3 \tanh\left(\hat{D}_3\right)\right)\frac{1}{\cosh^2\left(\hat{D}_3\right)}\dot{\hat{D}}_3 \end{aligned} \tag{40}$$

Inserting Eqs. (28) and (29) into (40) leading to the following result:

$$\begin{aligned} \dot{V}_3 \leq& -k_5 S_1 \operatorname{sign}\left(S_1\right) + \left|S_1\right| D_1 + \left|S_2\right| D_2 \\ &- \frac{k_6\left(m_{22}u_d - m_{11}u\right)S_2}{m_{33}}\operatorname{sign}\left(\frac{\left(m_{22}u_d - m_{11}u\right)S_2}{m_{33}}\right) \\ &- \frac{2\lambda_1}{\lambda_4}\left(\bar{D}_1 - \lambda_1 \tanh\left(\hat{D}_1\right)\right)\frac{1}{\cosh^2\left(\hat{D}_1\right)}\dot{\hat{D}}_1 \\ &- \frac{2\lambda_2}{\lambda_5}\left(\bar{D}_2 - \lambda_2 \tanh\left(\hat{D}_2\right)\right)\frac{1}{\cosh^2\left(\hat{D}_2\right)}\dot{\hat{D}}_2 \\ &- \frac{2\lambda_3}{\lambda_6}\left(\bar{D}_3 - \lambda_3 \tanh\left(\hat{D}_3\right)\right)\frac{1}{\cosh^2\left(\hat{D}_3\right)}\dot{\hat{D}}_3 \\ &- \lambda_1 \tanh\left(\hat{D}_1\right)\left|S_1\right| - \lambda_2 \tanh\left(\hat{D}_2\right)\left|S_2\right| \\ &- \lambda_3 \tanh\left(\hat{D}_3\right)\left|\frac{\left(m_{22}u_d - m_{11}u\right)S_2}{m_{33}}\right| \\ &+ \frac{\left|\left(m_{22}u_d - m_{11}u\right)S_2\right|}{m_{33}}D_3 \\ \leq& -k_5\left|S_1\right| - k_6\left|\frac{\left(m_{22}u_d - m_{11}u\right)S_2}{m_{33}}\right| \\ &- \frac{2\lambda_1}{\lambda_4}\left(\bar{D}_1 - \lambda_1 \tanh\left(\hat{D}_1\right)\right)\frac{1}{\cosh^2\left(\hat{D}_1\right)}\dot{\hat{D}}_1 \\ &- \frac{2\lambda_2}{\lambda_5}\left(\bar{D}_2 - \lambda_2 \tanh\left(\hat{D}_2\right)\right)\frac{1}{\cosh^2\left(\hat{D}_2\right)}\dot{\hat{D}}_2 \\ &- \frac{2\lambda_3}{\lambda_6}\left(\bar{D}_3 - \lambda_3 \tanh\left(\hat{D}_3\right)\right)\frac{1}{\cosh^2\left(\hat{D}_3\right)}\dot{\hat{D}}_3 \\ &+ \left|S_1\right|\tilde{D}_1 + \left|S_2\right|\tilde{D}_2 + \left|\frac{\left(m_{22}u_d - m_{11}u\right)S_2}{m_{33}}\right|\tilde{D}_3 \end{aligned} \tag{41}$$

According to the proposed adaptive laws Eqs (30)-(32), Eq. (41) can be further written as:

$$\begin{aligned} \dot{V}_3 \leq& -k_5\left|S_1\right| - k_6\left|\frac{\left(m_{22}u_d - m_{11}u\right)S_2}{m_{33}}\right| \\ &- 2\left(\bar{D}_1 - \lambda_1 \tanh\left(\hat{D}_1\right)\right)\left|S_1\right| \\ &- 2\left(\bar{D}_2 - \lambda_2 \tanh\left(\hat{D}_2\right)\right)\left|S_2\right| \\ &- 2\left(\bar{D}_3 - \lambda_3 \tanh\left(\hat{D}_3\right)\right)\left|\frac{\left(m_{22}u_d - m_{11}u\right)S_2}{m_{33}}\right| \\ &+ \left|S_1\right|\left(D_1 - \lambda_1 \tanh\left(\hat{D}_1\right)\right) \\ &+ \left|S_2\right|\left(D_2 - \lambda_2 \tanh\left(\hat{D}_2\right)\right) \\ &+ \left|\frac{\left(m_{22}u_d - m_{11}u\right)S_2}{m_{33}}\right|\left(D_3 - \lambda_3 \tanh\left(\hat{D}_3\right)\right) \end{aligned} \tag{42}$$

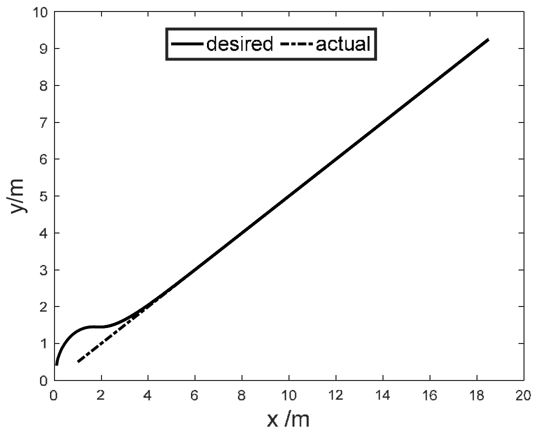

FIGURE 1. The actual and desired paths of the MSV.

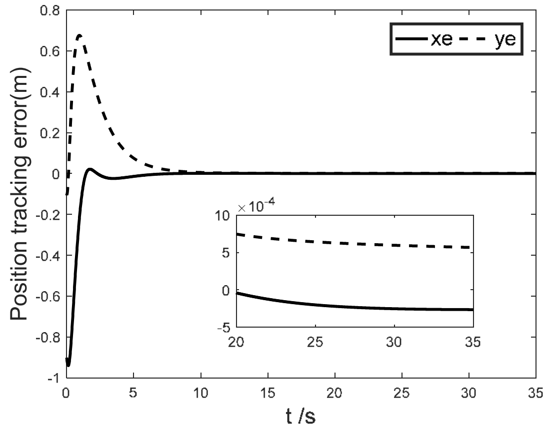

FIGURE 2. Curves of position tracking errors.

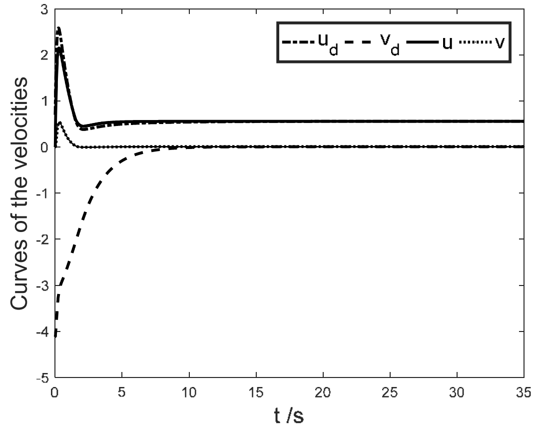

FIGURE 3. The practical and desired velocity of the MSV.

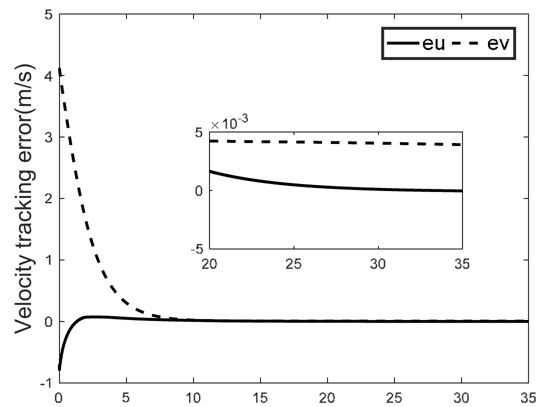

FIGURE 4. Curves of the velocity tracking errors.

Due to the fact that $\bar{D}_i > D_i$ and $\bar{D}_i > \lambda_i \tanh\left(\hat{D}_i\right)$, Eq. (42) finally becomes:

$$\begin{aligned}
\dot{V}_3 \leq& -k_5 |S_1| - k_6 \left|\frac{(m_{22}u_d - m_{11}u) S_2}{m_{33}}\right| \\
&- \left(\bar{D}_1 - \lambda_1 \tanh\left(\hat{D}_1\right)\right) |S_1| \\
&- \left(\bar{D}_2 - \lambda_2 \tanh\left(\hat{D}_2\right)\right) |S_2| \\
&- \left(\bar{D}_3 - \lambda_3 \tanh\left(\hat{D}_3\right)\right) \left|\frac{(m_{22}u_d - m_{11}u) S_2}{m_{33}}\right| \\
=& -2k_5 \left(\frac{1}{2}S_1^2\right)^{\frac{1}{2}} - 2k_6 \left|\frac{(m_{22}u_d - m_{11}u)}{m_{33}}\right| \left(\frac{1}{2}S_1^2\right)^{\frac{1}{2}} \\
&- \sqrt{\lambda_4}\, |S_1| \left(\frac{1}{\lambda_4}\left(\bar{D}_1 - \lambda_1 \tanh\left(\hat{D}_1\right)\right)^2\right)^{\frac{1}{2}} \\
&- \sqrt{\lambda_5}\, |S_2| \left(\frac{1}{\lambda_5}\left(\bar{D}_2 - \lambda_2 \tanh\left(\hat{D}_2\right)\right)^2\right)^{\frac{1}{2}} \\
&- \sqrt{\lambda_6} \left|\frac{(m_{22}u_d - m_{11}u) S_2}{m_{33}}\right| \\
&\left(\frac{1}{\lambda_6}\left(\bar{D}_3 - \lambda_3 \tanh\left(\hat{D}_3\right)\right)^2\right)^{\frac{1}{2}} \\
\leq& -\rho_5 V_3^{\frac{1}{2}} \qquad (43)
\end{aligned}$$

where

$$\rho_5 = \min\left(2k_5, 2k_6 \left|\frac{(m_{22}u_d - m_{11}u)}{m_{33}}\right|, \sqrt{\lambda_4}\, |S_1|, \sqrt{\lambda_5}\, |S_2|, \sqrt{\lambda_6} \left|\frac{(m_{22}u_d - m_{11}u) S_2}{m_{33}}\right|\right).$$

In view of Lemma 1, it comes to the conclusion that the sliding mode surface $S_i, i = 1, 2$ converges to the origin in finite time.

Now, point (i) has been proven.

When the motion of the tracking error system Eq. (7) reaches the sliding mode surface $S_i = 0, i = 1, 2$ and remains on it, Eqs. (44) and (45) can be obtained for e_u and e_v, respectively.

$$\dot{e}_u = -k_3 \tanh(\kappa e_u) \qquad (44)$$
$$\dot{e}_v = -k_4 \tanh(\kappa e_v) \qquad (45)$$

For the surge tracking error e_u, it can be concluded from $S_1 = 0$ that the relation $\dot{S}_1 = 0$ always exists. Accordingly, Eq. (44) is tenable. For the sway tracking error e_v, Eq. (45) is obviously valid from the equation $S_2 = 0$.

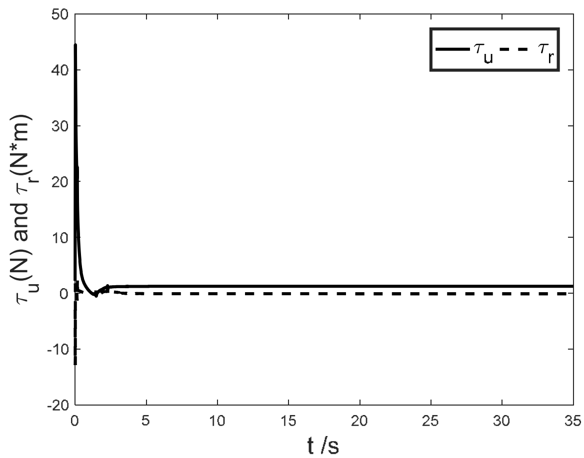

FIGURE 5. Curves of the control torques.

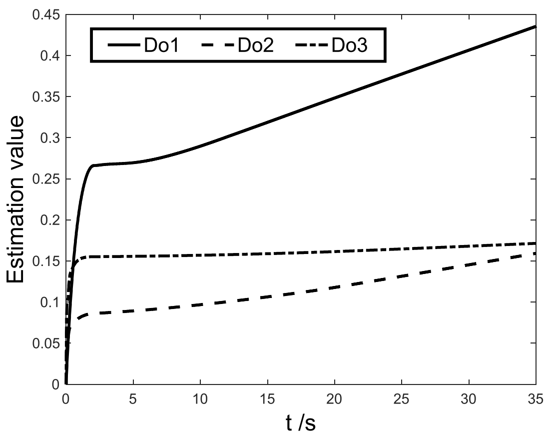

FIGURE 6. Curves of the estimation information.

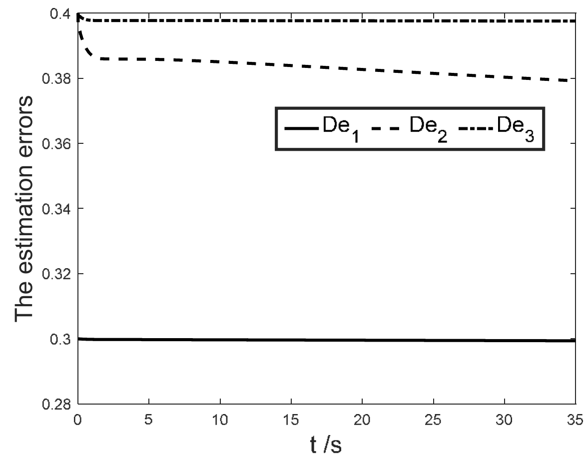

FIGURE 7. Curves of the estimation errors.

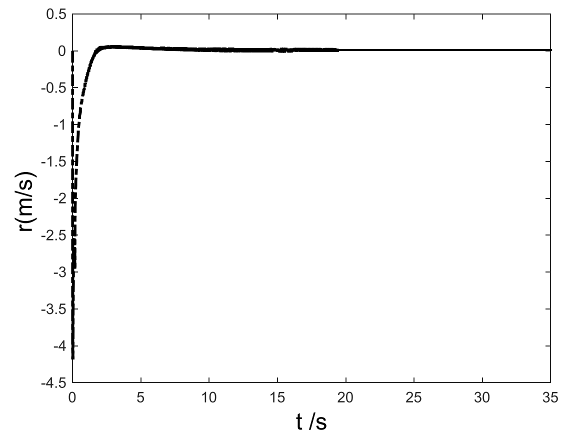

FIGURE 8. The curve of the yaw angular velocity.

To illustrate the finite-time stability of the tracking errors, the Lyapunov function is chosen as:

$$V_4 = \frac{1}{2}e_u^2 + \frac{1}{2}e_v^2 \tag{46}$$

By exploiting Eqs. (44), (45) and Lemma 3, the derivative of Eq. (46) is derived as;

$$\begin{aligned}\dot{V}_4 &= e_u\dot{e}_u + e_v\dot{e}_v \\ &= -k_3e_u\tanh(\kappa e_u) - k_4e_v\tanh(\kappa e_v) \\ &\le -k_3|e_u| - k_4|e_v| + k_3 + k_4 \\ &= -\sqrt{2}k_3\left(\frac{1}{2}e_u^2\right)^{\frac{1}{2}} - \sqrt{2}k_4\left(\frac{1}{2}e_v^2\right)^{\frac{1}{2}} + k_3 + k_4 \\ &= -\rho_6V_4^{\frac{1}{2}} + k_3 + k_4 \end{aligned} \tag{47}$$

where $\rho_6 = \min\left(\sqrt{2}\,k_3, \sqrt{2}\,k_4\right)$. Then, it can be followed from Lemma 1 and Lemma 2 that e_u and e_v will converge to the region Δ_u and Δ_v in finite time.

Now, point (ii) has been proven.

Now, Theorem 2 has been proven.

IV. SIMULATION RESULTS

In this section, the effectiveness of the proposed control scheme will be illustrated by numerical simulations. The model parameters of an underactuated surface vessel is given as [15]: $m_{11} = 1.9 \pm 0.019$kg,$m_{22} = 2.4 \pm 0.117$kg, $m_{33} = 0.043$kg $\pm\, 0.0068$, $d_{11} = 2.436 \pm 0.0023$, $d_{22} = 12.9 \pm 0.297$, $d_{33} = 0.0564 \pm 0.00085$. The initial conditions of the MSV are set as: $x(0) = 0.1, y(0) = 0.4$, $\varphi(0) = \frac{\pi}{2}, u(0) = 0, v(0) = 0, r(0) = 0$. The reference trajectory is chosen as: $x_d(t) = 0.5t + 1m$, $y_d(t) = 0.25t + 0.5m$. To testify the robustness of the proposed controller, the following disturbance is considered in the simulation: $\tau_{ud} = 0.1 \times \left(1 + 0.2\sin\left(0.01\text{t} + \frac{\pi}{2}\right)\right)$, $\tau_{vd} = 0.1 \times (1 + 0.3\cos(0.01\text{t}))$, $\tau_{rd} = 0.1 \times (1 + 0.2\cos(0.015\text{t}))$.

The design parameters are selected as: $k_1 = 2, k_2 = 2$, $k_3 = 0.2, k_4 = 2, k_5 = 0.05, k_6 = 0.05, k_7 = 3, k_8 = 3$, $\lambda_1 = 0.01$, $\lambda_2 = 0.01$, $\lambda_3 = 0.01, \lambda_4 = 0.0005, \lambda_5 = 1$, $\lambda_6 = 0.01$.Simulation results are depicted in Figs. 1-8. In Fig.1, the actual path of the MSV is presented along with the desired one. Obviously, the desired path can be tracked by the MSV with high control precision. The position tracking error curves are given in Fig. 2, implying that the desired position trajectory can be tracked within 6s even in the pres-

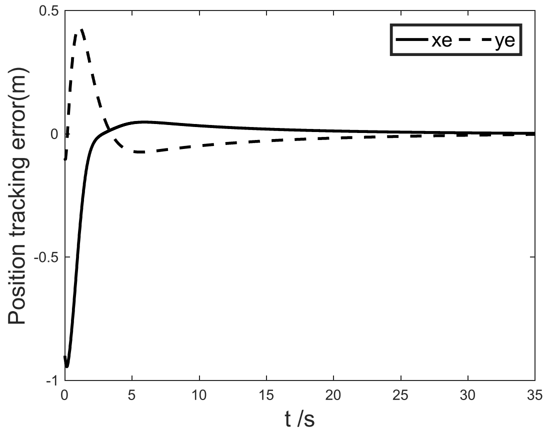

FIGURE 9. Curves of position tracking errors under the controller Eq. (19) in [14].

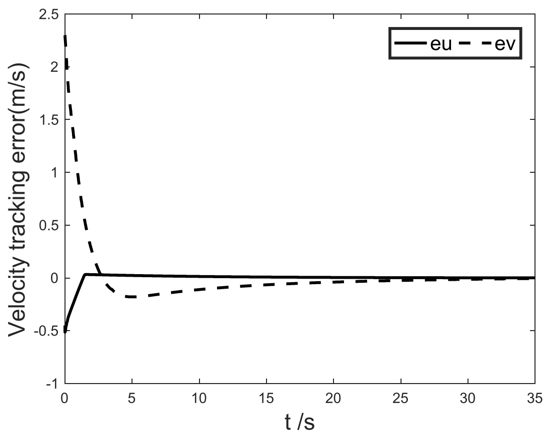

FIGURE 10. Curves of the velocity tracking errors under the controller Eq. (19) in [14].

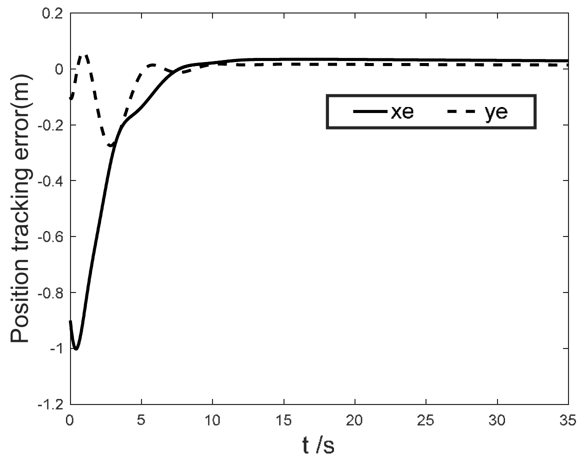

FIGURE 11. Curves of position tracking errors under the controller Eqs. (22)-(23) in [15].

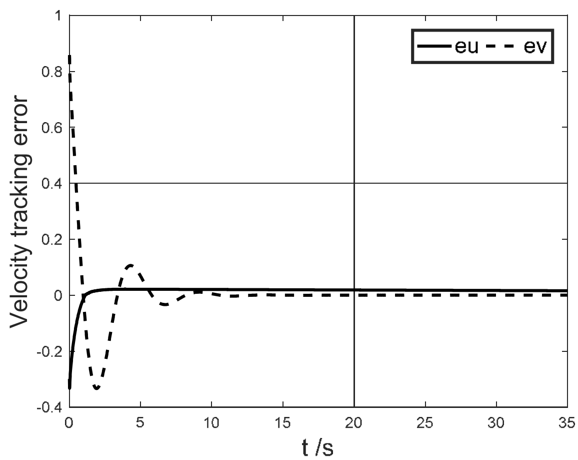

FIGURE 12. Curves of velocity tracking errors under the controller Eqs. (22)-(23) in [15].

ence of external disturbance and parameter uncertainties. The practical and desired velocity of the MSV are described in Fig. 3. It can be founded that the proposed velocity command described as Eq. (8) can be tracked within 6s, which indicates the validity of Theorem 2. Curves of velocity tracking errors are given in Fig. 4. Steady-state errors of position and velocity can be observed from enlarged pictures in Fig. 2 and Fig. 4, respectively. Curves of the control torque are given in Fig. 5. According to the designed control law Eqs. (28) and (29), it is obviously that the sign function will introduce chattering problem in the MSV system. To solve this problem, the boundary layer function is introduced in the numerical simulations. The estimation information is depicted in Fig. 6, which shows that estimation values are all bounded. To illustrate that $\tilde{D}_i$ is bounded, Fig. 7 shows the estimation error curves. Fig. 8 depicts the curve of the yaw angular velocity r. It can be observed that the yaw angular velocity is always bounded under the proposed control law.

To better show the effectiveness of the proposed control scheme, the comparative study with sliding mode controllers proposed in [14] and [15] is made. Taking the same external disturbance into account, simulation results of [14] and [15] are given in Figs. 9-12. Comparing the simulation results under different controllers, it can be concluded that the proposed controller in this paper possesses faster convergence rate and higher control precision.

V. CONCLUSIONS

The robust finite-time trajectory tracking control problem has been solved for underactuated MSVs in this paper by employing finite-time sliding mode control technology. The controller design can be divided into two stages: the desired velocity design and the finite-time controller design. A novel sliding mode surface has been proposed such that the position tracking errors can be stabilized within finite time. Numerical simulations have shown the effectiveness of the proposed method.

REFERENCES

[1] Z. Zheng, Y. Huang, L. Xie, and B. Zhu, "Adaptive trajectory tracking control of a fully actuated surface vessel with asymmetrically constrained input and output," *IEEE Trans. Control Syst. Technol.*, vol. 26, no. 5, pp. 1851–1859, Sep. 2018.

[2] N. Khaled and N. G. Chalhoub, "A dynamic model and a robust controller for a fully-actuated marine surface vessel," *J. Vib. Control*, vol. 17, no. 6, pp. 801–812, 2011.
[3] H. Xin and J. Du, "Robust nonlinear control design for dynamic positioning of marine vessels with thruster system dynamics," *Nonlinear Dyn.*, vol. 94, no. 1, pp. 365–376, 2018.
[4] S.-L. Dai, S. He, H. Lin, and C. Wang, "Platoon formation control with prescribed performance guarantees for USVs," *IEEE Trans. Ind. Electron.*, vol. 65, no. 5, pp. 4237–4246, May 2018.
[5] Y. Lu, G. Zhang, Z. Sun, and W. Zhang, "Adaptive cooperative formation control of autonomous surface vessels with uncertain dynamics and external disturbances," *Ocean Eng.*, vol. 167, pp. 36–44, Nov. 2018.
[6] Z. Zheng, L. Sun, and L. Xie, "Error-constrained LOS path following of a surface vessel with actuator saturation and faults," *IEEE Trans. Syst., Man, Cybern. Syst.*, vol. 48, no. 10, pp. 1794–1805, Oct. 2018.
[7] Y. Guo, B. Huang, A.-J. Li, and C.-Q. Wang, "Integral sliding mode control for Euler-Lagrange systems with input saturation," *Int. J. Robust Nonlinear Control*, vol. 29, no. 4, pp. 1088–1100, 2019.
[8] B. Huang, A. J. Li, Y. Guo, and C.-Q. Wang, "Rotation matrix based finite-time attitude synchronization control for spacecraft with external disturbances," *ISA Trans.*, vol. 85, pp. 141–150, Feb. 2019.
[9] B. Huang, A. Li, Y. Guo, and C.-Q. Wang, "Fixed-time attitude tracking control for spacecraft without unwinding," *Acta Astron.*, vol. 151, pp. 818–827, Oct. 2018.
[10] M. Van, "Adaptive neural integral sliding-mode control for tracking control of fully actuated uncertain surface vessels," *Int. J. Robust Nonlinear Control*, vol. 29, no. 5, pp. 1537–1557, 2019.
[11] M. Van, "An enhanced tracking control of marine surface vessels based on adaptive integral sliding mode control and disturbance observer," *ISA Trans.*, to be published. doi: 10.1016/j.isatra.2018.12.047.
[12] Z. Zhao, W. He, and S. S. Ge, "Adaptive neural network control of a fully actuated marine surface vessel with multiple output constraints," *IEEE Trans. Control Syst. Technol.*, vol. 22, no. 4, pp. 1536–1543, Jul. 2014.
[13] L. Kong, W. He, C. Yang, G. Li, and Z. Zhang, "Adaptive fuzzy control for a marine vessel with time-varying constraints," *IET Control Theory Appl.*, vol. 12, no. 10, pp. 1448–1455, Mar. 2018.
[14] T. Elmokadem, M. Zribi, and K. Youcef-Toumi, "Trajectory tracking sliding mode control of underactuated AUVs," *Nonlinear Dyn.*, vol. 84, no. 2, pp. 1079–1091, Apr. 2016.
[15] R. Yu, Q. Zhu, G. Xia, and Z. Liu, "Sliding mode tracking control of an underactuated surface vessel," *IET Control Theory Appl.*, vol. 6, no. 3, pp. 461–466, 2012.
[16] Z. Yan, M. Wang, and J. Xu, "Robust adaptive sliding mode control of underactuated autonomous underwater vehicles with uncertain dynamics," *Ocean Eng.*, vol. 173, pp. 802–809, Feb. 2019.
[17] O. Elhaki and K. Shojaei, "Neural network-based target tracking control of underactuated autonomous underwater vehicles with a prescribed performance," *Ocean Eng.*, vol. 167, pp. 239–256, Nov. 2018.
[18] S. L. Dai, S. He, and H. Lin, "Transverse function control with prescribed performance guarantees for underactuated marine surface vehicles," *Int. J. Robust Nonlinear Control*, vol. 29, no. 5, pp. 1577–1596, 2019.
[19] Z. Jia, Z. Hu, and W. Zhang, "Adaptive output-feedback control with prescribed performance for trajectory tracking of underactuated surface vessels," *ISA Trans.*, to be published. doi: 10.1016/j.isatra.2019.04.035.
[20] J. Ghommam, S. El Ferik, and M. Saad, "Robust adaptive path-following control of underactuated marine vessel with off-track error constraint," *Int. J. Syst. Sci.*, vol. 49, no. 7, pp. 1540–1558, Mar. 2018.
[21] K. Shojaei, "Leader–follower formation control of underactuated autonomous marine surface vehicles with limited torque," *Ocean Eng.*, vol. 105, pp. 196–205, Sep. 2015.
[22] Y. Lu, G. Zhang, L. Qiao, and W. Zhang, "Adaptive output-feedback formation control for underactuated surface vessels," *Int. J. Control*, to be published.
[23] S. J. Yoo and B. S. Park, "Guaranteed performance design for distributed bounded containment control of networked uncertain underactuated surface vessels," *J. Franklin Inst.*, vol. 354, no. 3, pp. 1584–1602, 2017.
[24] J. Ghommam and M. Saad, "Adaptive leader–follower formation control of underactuated surface vessels under asymmetric range and bearing constraints," *IEEE Trans. Veh. Technol.*, vol. 67, no. 2, pp. 852–865, Feb. 2018.
[25] J. Ghommam and M. Saad, "Backstepping-based cooperative and adaptive tracking control design for a group of underactuated AUVs in horizontal plan," *Int. J. Control*, vol. 87, no. 5, pp. 1076–1093, 2014.
[26] M. Fu and L. Yu, "Finite-time extended state observer-based distributed formation control for marine surface vehicles with input saturation and disturbances," *Ocean Eng.*, vol. 159, pp. 219–227, Jul. 2018.
[27] L. Yu and M. Fu, "A robust finite-time output feedback control scheme for marine surface vehicles formation," *IEEE Access*, vol. 6, pp. 41291–41301, 2018.
[28] X. Jin, "Fault tolerant finite-time leader-follower formation control for autonomous surface vessels with LOS range and angle constraints," *Automatica*, vol. 68, pp. 228–236, Jun. 2016.
[29] J. Zhang, S. Yu, and Y. Yan, "Fixed-time output feedback trajectory tracking control of marine surface vessels subject to unknown external disturbances and uncertainties," *ISA Trans.*, to be published. doi: 10.1016/j.isatra.2019.03.007.
[30] M. Fu, T. Wang, and C. Wang, "Adaptive neural-based finite-time trajectory tracking control for underactuated marine surface vessels with position error constraint," *IEEE Access*, vol. 7, pp. 16309–16322, 2019.
[31] T. Elmokadema, M. Zribia, and K. Youcef-Toumi, "Terminal sliding mode control for the trajectory tracking of underactuated autonomous underwater vehicles," *Ocean Eng.*, vol. 129, pp. 613–625, Jan. 2017.

LEI ZHANG received the bachelor's and Ph.D. degrees in engineering from Harbin Engineering University, in 2004 and 2011, respectively, where he is currently an Associate Professor and the Director of the Unmanned Surface Vehicle Technology Research and Development Center. His research interests include robust control, nonlinear control for marine surface vessels, formation tracking control for underwater vehicles, fault-tolerant control, sliding mode control, and intelligent control.

BING HUANG received the bachelor's degree from the Nanjing University of Aeronautics and Astronautics, in 2013, and the master's and Ph.D. degrees from Northwestern Polytechnical University, in 2015 and 2019, respectively. He is currently a Lecturer with Harbin Engineering University. His research interests include robust control, nonlinear control for marine surface vessels, formation tracking control for underwater vehicles, fault-tolerant control, sliding mode control, and intelligent control.

YULEI LIAO was born in Chongqing, China, in 1985. He received the B.Eng. degree in naval architecture and ocean engineering and the Ph.D. degree in design and manufacture of marine structures from Harbin Engineering University, Harbin, China, in 2007 and 2012, respectively, where he has been an Associate Professor with the College of Shipbuilding Engineering, since 2016. From 2013 to 2016, he was a Research Assistant with the Science and Technology on Underwater Vehicle Laboratory. He is the author of one book, more than 40 articles, and more than 50 inventions. His research interests include intelligent marine vehicles, marine vehicles swarming, ocean energy driving marine vehicles, new-concept marine vehicles, and intelligent motion control.

BO WANG received the bachelor's degree from Tsinghua University, the master's degree from Bauman Moscow State Technical University, and the Ph.D. degree from Harbin Engineering University. He is currently an Associate Professor with the Unmanned Surface Vehicle Technology Research and Development Center, Harbin Engineering University. His research interests include intelligent sensing technology of marine environment, machine learning and pattern recognition techniques, deep learning for unmanned systems, and intelligent control.